

Multicomponent Reassembly of Terpyridine-based Materials: Quantitative Metallomacrocyclic Rearrangement

Rajarshi Sarkar,[†] Zaihong Guo,[‡] Jingyi Li,[‡] Tarak N. Burai,[‡] Charles N. Moorefield,[‡]
Chrys Wesdemiotis,^{*†‡} and George R. Newkome^{*†‡}

[†]Department of Chemistry and [‡]Department of Polymer Science, The University of Akron, Akron, Ohio-44325

Table of contents

Experimental Section.....	S1
General Procedure.....	S1-S4
NMR Spectra of complexes.....	S5-S12
ESI, TWIM spectra and ESI-gMS² plot of complexes.....	S13-S16

Experimental Section

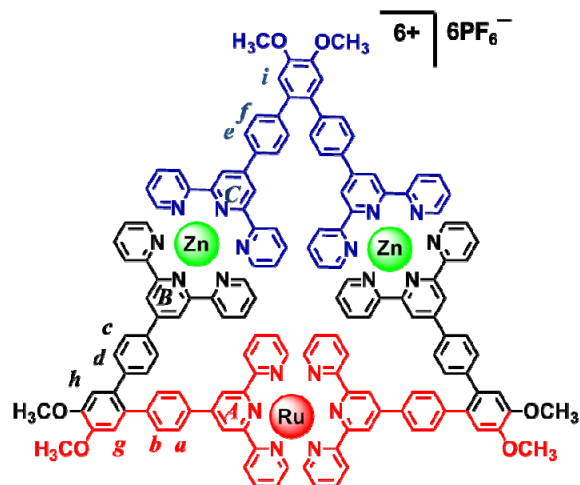
General Procedures. Reagents and solvents were purchased from Sigma-Aldrich and used without purification. Thin layer chromatography (TLC) was performed on flexible sheets (Baker-flex) precoated with Al₂O₃ (IB-F) or SiO₂ (IB2-F) and visualized by UV light. Column chromatography was conducted using basic Al₂O₃, Brockman Activity I (60-325 mesh) or SiO₂ (60-200 mesh) from Fisher Scientific. ¹H, ¹³C, ²D COSY, and NOESY NMR spectra were recorded on a Varian NMR 500. ESI mass spectrometry (MS) experiments were performed on a Waters Synapt HDMS quadrupole/time-of-flight (Q/ToF) tandem mass spectrometer. This instrument contains a triwave device between the Q and ToF analyzers, consisting of three collision cells in the order trap cell, ion mobility cell, and transfer cell. Trap and transfer cells are pressurized with Ar, and the ion mobility cell is pressurized with N₂ flowing in a direction opposite to that of the entering ions. In TWIM experiments, a pulsed field is applied to the ion mobility cell ("traveling wave" field) to separate the ions drifting inside it by their charge state and collision cross-section. The ESI-TWIM-MS experiments were performed using the following parameters: ESI capillary voltage: 1.0 kV; sample cone voltage: 8 V; extraction cone voltage: 3.2 V; desolvation gas flow: 800 L h⁻¹ (N₂); trap collision energy (CE): 1 eV; transfer CE: 1 eV; trap gas flow: 1.5 mL min⁻¹ (Ar); ion-mobility cell gas flow: 22.7 mL min⁻¹(N₂); sample flow rate: 5 μL min⁻¹; source temperature: 30 °C; desolvation temperature: 40 °C; TWIM traveling-wave height: 7.5 V; and TWIM traveling-wave velocity: 350 ms⁻¹. The sprayed solution was prepared by dissolving the sample (300 μg) in a mixture of MeCN/MeOH (1 mL; 1:1, v/v). In the gMS² tandem MS experiments, a specific complex ion was mass-selected by Q and underwent collisionally activated dissociation with Ar gas in the trap cell; the ion abundances around the *m/z* value of the mass-selected complex ion were monitored after IM separation and ToF mass analysis, as the trap CE was gradually increased until the complex ion dissociated completely. The center-of-mass collision energy (E_{COM}) of disappearance of the

complex ion was calculated from the corresponding laboratory-frame collision energy (E_{LAB}) using the equation $E_{\text{COM}} = E_{\text{LAB}} [m_{\text{gas}}/(m_{\text{gas}}+m_{\text{ion}})]$, where m_{gas} and m_{ion} are the masses of the collision gas in the trap cell (Ar, 40 Da) and of the selected complex ion, respectively. Note that a voltage bias of 20 V on the trap cell provides a collision energy of $20z$ eV, where z is the ion charge. Similarly, the mass of an ion in charge state $+z$ is calculated by multiplying the mass-to-charge ratio of the ion by z . Data analyses were conducted using the MassLynx 4.1 and DriftScope 2.1 programs provided by Waters. Photoluminescence spectra were collected by using a Horiba Jobin Yvon FluoroMax-4 fluorometer. The excitation and emission monochromators were set at 5 and 2 nm, respectively, giving a spectral bandwidth of 4.25 nm. Quartz cell with 1 cm path length was used for all the experiments. The data interval was 0.5 nm and the integration time was 2.0 sec. MeCN was used to prepare the solution for complexes and CHCl_3 for ligand. Absorbance of the samples was kept <0.1 at the 480 nm excitation wavelength to avoid any inner-filter effect. The dark counts were subtracted and the spectra were corrected for wavelength-dependent instrument sensitivity.

Synthesis of bimetallic triangle [(1)(2)(Zn²⁺)₂] (PF₆⁻)₆ (7):

Method A: To a MeOH solution of triangle **3**^[1] [(1)₃Zn₃²⁺] (NO₃⁻)₆ (10 mg, 3.53×10^{-3} mmol), a MeOH solution of tetramer **5** [(2)₂(Zn²⁺)₂] (NO₃⁻)₈^[2] (20.35 mg, 5.30×10^{-3} mmol, 1.5 eq) was added. The solution was stirred for 30 minutes at 25 °C. Then excess NH₄PF₆ was added to obtain a light orange precipitate, which was filtered and washed repeatedly with MeOH to remove excess NH₄PF₆. The product **7** was obtained (98%) as an orange solid: 35.02 mg; mp > 300 °C.

Method B: To a solution of ligand **1**^[3] (5 mg, 6.64×10^{-3} mmol) and dimer **2**^[4] (11.49 mg, 6.64×10^{-3} mmol) in CHCl_3 (10 mL), a MeOH solution (5 mL) of Zn(NO₃)₂·6H₂O (3.95 mg, 13.28×10^{-3} mmol) was added. The solution was stirred for 30 minutes at 25 °C. Then excess NH₄PF₆ was added to obtain a light orange precipitate, which was filtered and washed repeatedly with MeOH to give (98%) **7**, as an orange solid: 21.87 mg; mp > 300 °C.

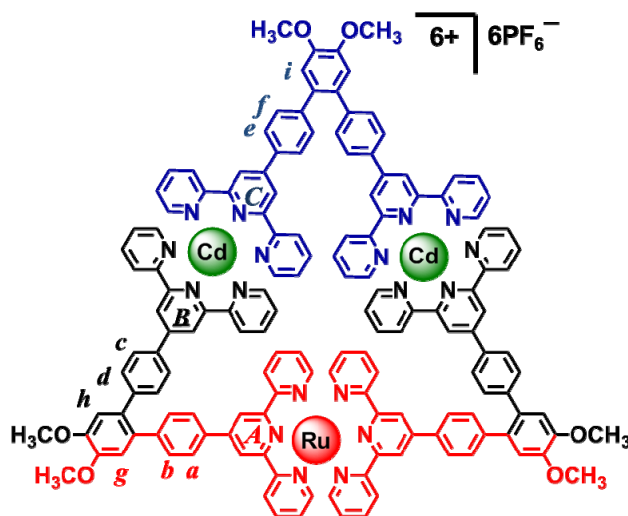


^1H NMR (CD_3CN , 500 MHz, ppm): δ 9.00 (s, 4H, $\text{tpy}^A\text{H}^{3',5'}$), 8.98 (s, 4H, $\text{tpy}^B\text{H}^{3',5'}$), 8.87 (s, 4H, $\text{tpy}^C\text{H}^{3',5'}$), 8.72 (d, $J = 8.0$ Hz, 4H, $\text{tpy}^C\text{H}^{3,3''}$), 8.70 (d, $J = 8.0$ Hz, 4H, $\text{tpy}^B\text{H}^{3,3''}$), 8.64 (d, $J = 8.0$ Hz, 4H, $\text{tpy}^A\text{H}^{3,3''}$), 8.14 (m, 12H, Ar-H^a , Ar-H^c , Ar-H^e), 8.08 (t, 8H, $\text{tpy}^B\text{H}^{4,4''}$, $\text{tpy}^C\text{H}^{4,4''}$), 7.83 (m, 12H, $\text{tpy}^A\text{H}^{4,4''}$, $\text{tpy}^B\text{H}^{6,6''}$, $\text{tpy}^C\text{H}^{6,6''}$), 7.62 (m, 12H, Ar-H^b , Ar-H^d , Ar-H^f), 7.42 (d, $J = 5.0$ Hz, 4H, $\text{tpy}^A\text{H}^{6,6''}$), 7.35 (m, 8H, $\text{tpy}^B\text{H}^{5,5''}$, $\text{tpy}^C\text{H}^{5,5''}$), 7.26 (s, 2H, Ar-H^g), 7.25 (s, 2H, Ar-H^h), 7.23 (s, 2H, Ar-H^i), 7.13 (dd, $J_1 = 8.0$ Hz, $J_2 = 5.0$ Hz, 4H, $\text{tpy}^A\text{H}^{5,5''}$), 4.03 (s, 6H, Ar-OCH_3), 4.02 (s, 6H, Ar-OCH_3), 4.01 (s, 6H, Ar-OCH_3). ^{13}C NMR (CD_3CN , 125 MHz, ppm): 157.28, 154.83, 154.49, 151.47, 148.86, 148.41, 148.35, 147.05, 146.96, 146.74, 143.54, 143.42, 142.59, 140.27, 137.06, 133.98, 133.33, 133.27, 131.13, 130.96, 130.90, 130.42, 126.85, 126.81, 126.60, 126.57, 126.50, 123.66, 122.33, 120.43, 113.24, 54.84. ESI-MS (m/z): 1534.9 [$\text{M}-2\text{PF}_6^-$] $^{2+}$ (calculated $m/z = 1533.2$), 975.3 [$\text{M}-3\text{PF}_6^-$] $^{3+}$ (calculated $m/z = 973.8$), 695.2 [$\text{M}-4\text{PF}_6^-$] $^{4+}$ (calculated $m/z = 694.2$), 527.2 [$\text{M}-5\text{PF}_6^-$] $^{5+}$ (calculated $m/z = 526.3$), 415.1 [$\text{M}-6\text{PF}_6^-$] $^{6+}$ (calculated $m/z = 414.4$).

Synthesis of bimetallic triangle [(1)(2)(Cd^{2+}) $_2$] (PF_6^-) $_6$ (**8**):

Method A: To a MeOH solution of triangle **4**^[1] [(1) $_3\text{Cd}_3^{2+}$] (NO_3^-) $_6$ (10 mg, 3.36×10^{-3} mmol), a MeOH solution of tetramer **6**^[2] [(2) $_2(\text{Cd}^{2+})_2$] (NO_3^-) $_8$ (19.81 mg, 5.04×10^{-3} mmol, 1.5eqv) was added. The solution was stirred for 30 minutes at 25 °C. Then excess NH_4PF_6 was added to obtain a light orange precipitate, which was filtered and washed repeatedly with MeOH. The product **8** was obtained (99%) as an orange solid: 34.67 mg; mp > 300 °C.

Method B: To a solution of ligand **1** (5 mg, 6.64×10^{-3} mmol) and dimer **2** (11.49 mg, 6.64×10^{-3} mmol) in CHCl_3 (10 mL), a MeOH solution (5 mL) of $\text{Cd}(\text{NO}_3)_2 \cdot 4\text{H}_2\text{O}$ (4.10 mg, 13.28×10^{-3} mmol) was added. The solution was stirred for 30 minutes at 25 °C. Then excess NH_4PF_6 was added to obtain a light orange precipitate, which was filtered and washed repeatedly with MeOH. The product **8** was obtained (99%) as an orange solid: 22.67 mg; mp > 300 °C.



^1H NMR (CD_3CN , 500 MHz, ppm): δ 9.00 (s, 4H, $\text{tpy}^A\text{H}^{3',5'}$), 8.94 (s, 4H, $\text{tpy}^B\text{H}^{3',5'}$), 8.92 (s, 4H, $\text{tpy}^C\text{H}^{3',5'}$), 8.75 (t, 8H, $\text{tpy}^B\text{H}^{3,3''}$, $\text{tpy}^C\text{H}^{3,3''}$), 8.63 (d, $J = 8.0$ Hz, 4H, $\text{tpy}^A\text{H}^{3,3''}$), 8.10 (m, 28H, Ar-H^a , Ar-H^c , Ar-H^e , $\text{tpy}^B\text{H}^{4,4''}$, $\text{tpy}^C\text{H}^{4,4''}$, $\text{tpy}^B\text{H}^{6,6''}$, $\text{tpy}^C\text{H}^{6,6''}$), 7.86 (dd, $J_1 = J_2 = 8.0$ Hz, 4H, $\text{tpy}^A\text{H}^{4,4''}$), 7.64 (m, 12H, ArH^b , ArH^d , ArH^f), 7.47 (m, 8H, $\text{tpy}^A\text{H}^{6,6''}$, $\text{tpy}^B\text{H}^{5,5''}$, $\text{tpy}^C\text{H}^{5,5''}$), 7.28 (s, 2H, ArH^g), 7.26 (s, 2H, ArH^h), 7.24 (s, 2H, ArH^i), 7.17 (dd, $J_1 = 8.0$ Hz, $J_2 = 5.0$ Hz, 4H, $\text{tpy}^A\text{H}^{5,5''}$), 4.06 (s, 6H, ArOCH_3), 4.05 (s, 6H, ArOCH_3), 4.04 (s, 6H, ArOCH_3). ^{13}C NMR (CD_3CN , 125 MHz, ppm): 157.34, 154.56, 153.88, 151.52, 149.40, 148.76, 148.47, 148.43, 147.96, 146.79, 143.47, 143.36, 142.72, 140.35, 137.11, 133.98, 133.38, 131.07, 130.45, 130.40, 130.42, 126.82, 126.77, 126.52, 126.43, 123.70, 122.84, 120.78, 120.52, 113.47, 113.40, 113.36, 54.97, 54.95. ESI-MS (m/z): 1582.4 [$\text{M}-2\text{PF}_6$] $^{2+}$ (calculated $m/z = 1583.2$), 1006.9 [$\text{M}-3\text{PF}_6$] $^{3+}$ (calculated $m/z = 1007.2$), 718.2 [$\text{M}-4\text{PF}_6$] $^{4+}$ (calculated $m/z = 719.1$), 546.8 [$\text{M}-5\text{PF}_6$] $^{5+}$ (calculated $m/z = 546.3$), 430.1 [$\text{M}-6\text{PF}_6$] $^{6+}$ (calculated $m/z = 431.1$).

NMR spectra of ligands and complexes

Figure S1: ^1H NMR spectrum of triangle $[(1)_3(\text{Zn}^{2+})_3](\text{PF}_6^-)_6$ (3)

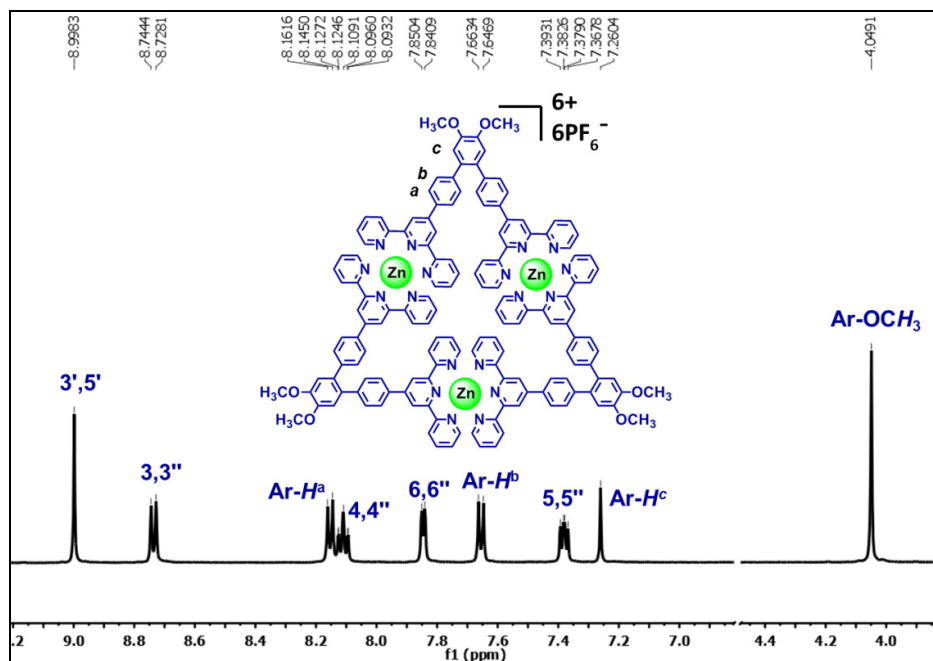


Figure S2: ^1H NMR spectrum of triangle $[(1)_3(\text{Cd}^{2+})_3](\text{PF}_6^-)_6$ (4)

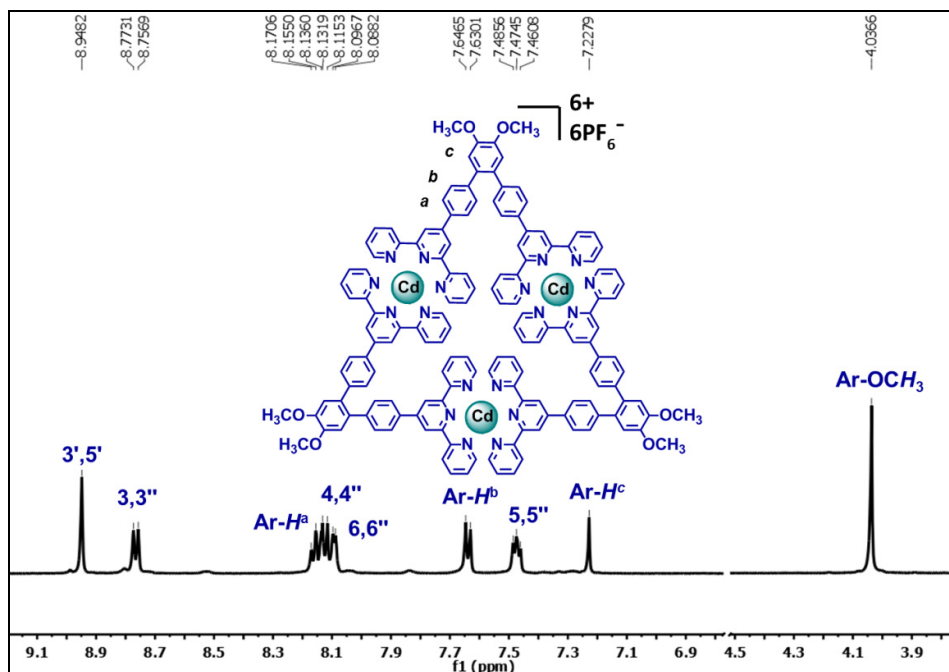


Figure S3: ^1H NMR spectrum of tetramer $[(\mathbf{2})_2(\text{Zn}^{2+})_2](\text{PF}_6^-)_8$ (**5**):

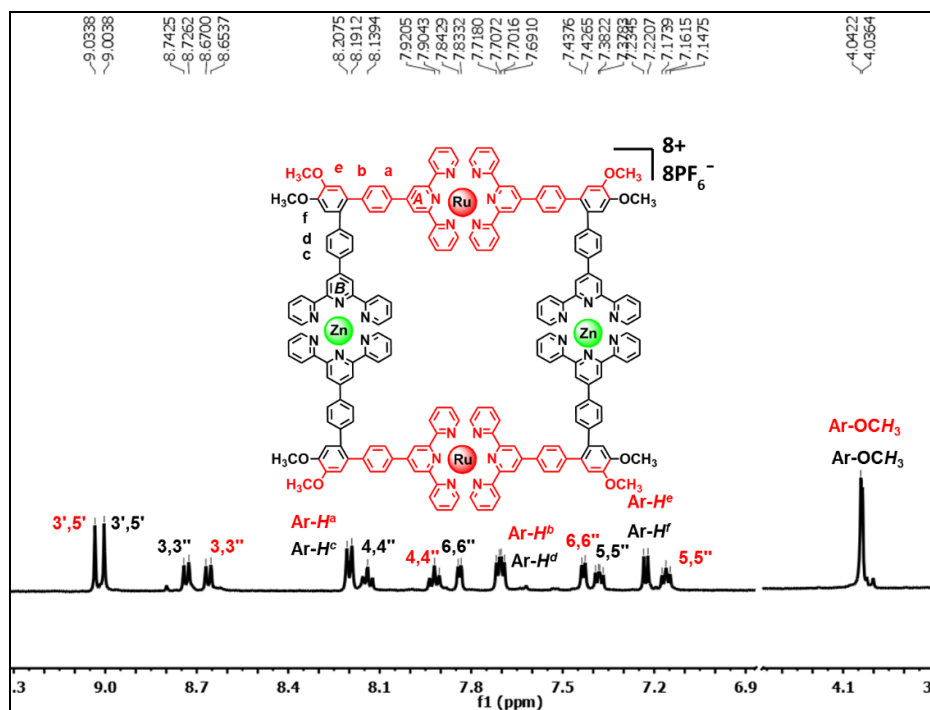


Figure S4: ^1H NMR spectrum of tetramer $[(\mathbf{2})_2(\text{Cd}^{2+})_2](\text{PF}_6^-)_8$ (**6**):

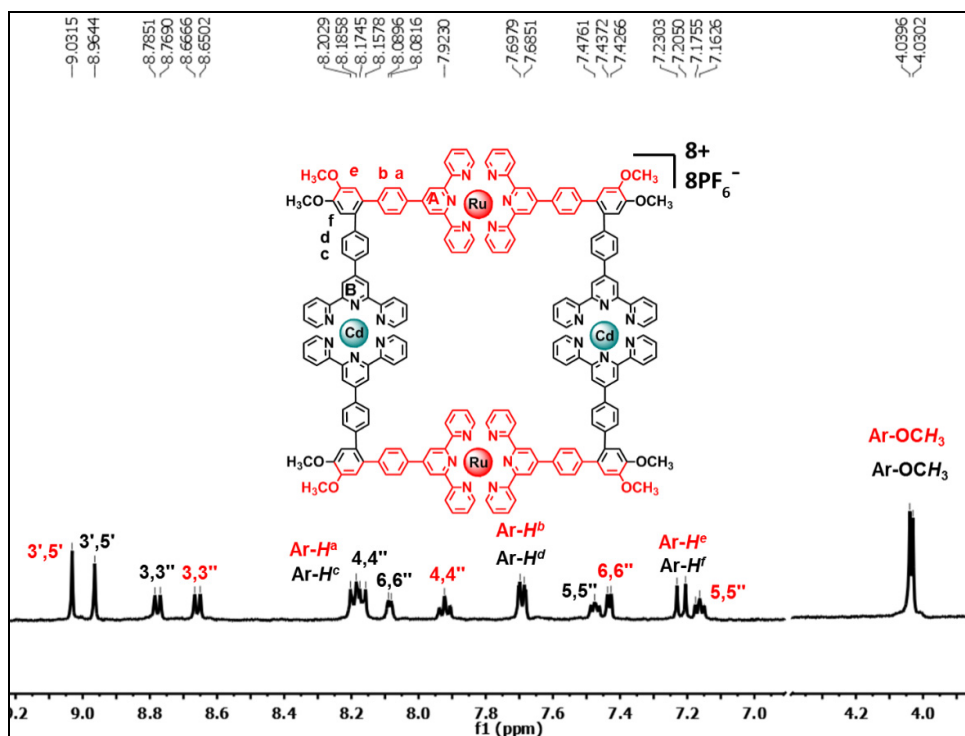


Figure S5: ^1H NMR spectrum of isosceles triangle $[(1)(2)(\text{Zn}^{2+})_2](\text{PF}_6^-)_6$ (**7**)

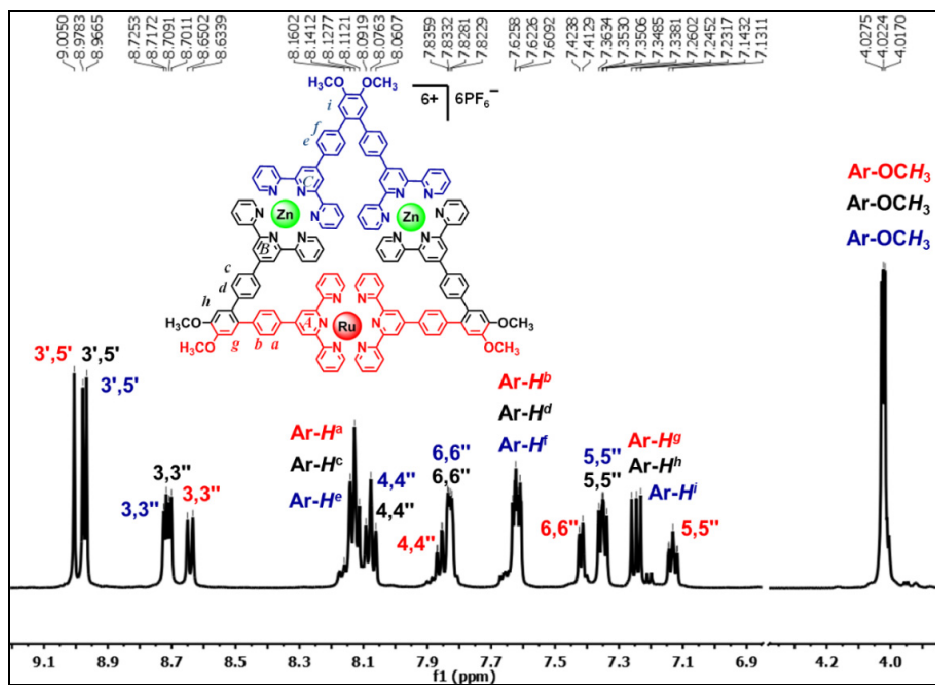


Figure S6: 2D COSY spectrum of isosceles triangle $[(1)(2)(\text{Zn}^{2+})_2](\text{PF}_6^-)_6$ (**7**)

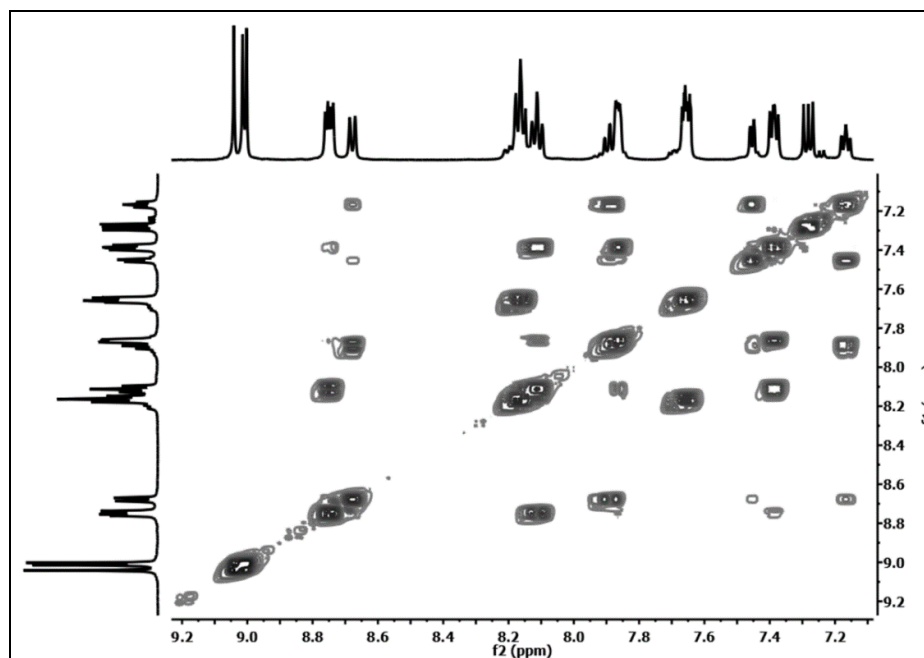


Figure S7: 2D NOESY spectrum of isosceles triangle [(1)(2)(Zn²⁺)₂] (PF₆⁻)₆ (7)

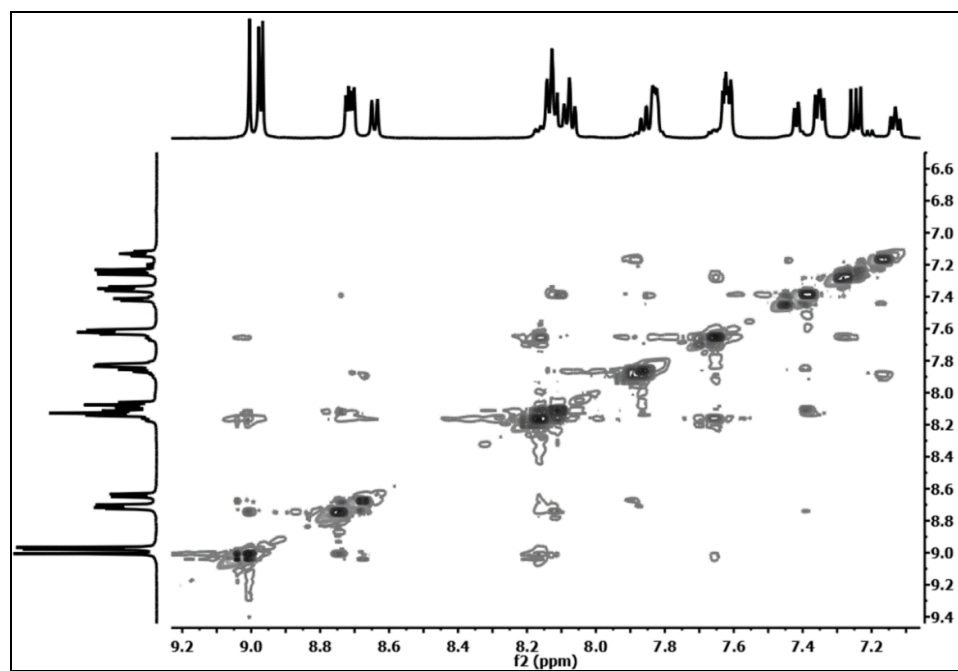


Figure S8: ¹³C NMR spectrum of isosceles triangle [(1)(2)(Zn²⁺)₂] (PF₆⁻)₆ (7)

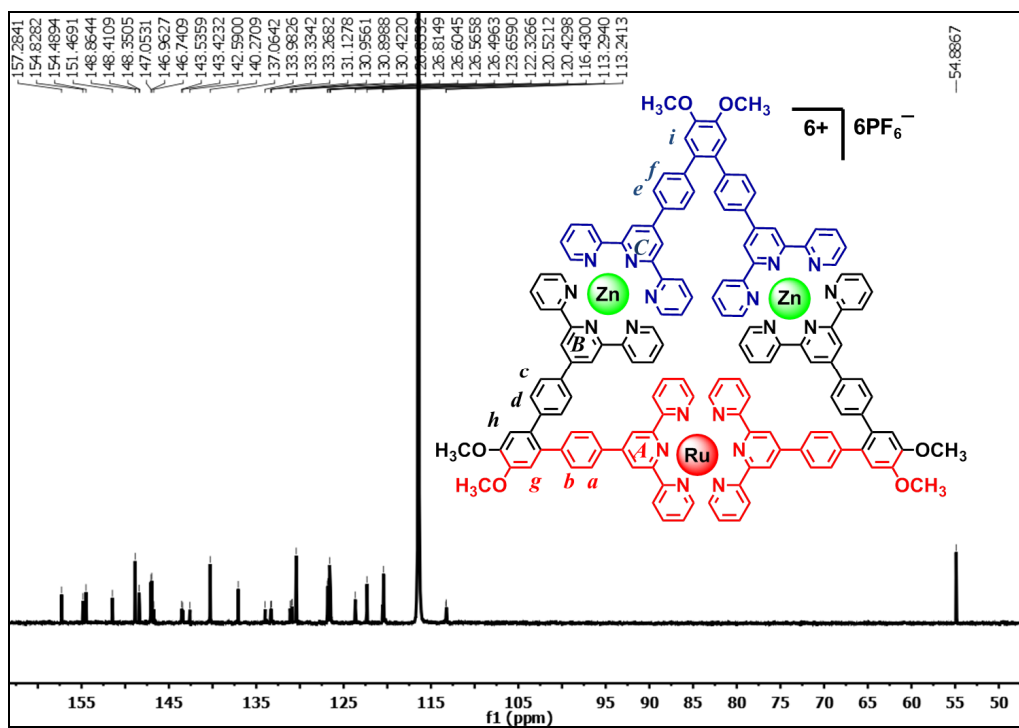


Figure S9: ^1H NMR spectrum of isosceles triangle $[(1)(2)(\text{Cd}^{2+})_2](\text{PF}_6^-)_6$ (**8**)

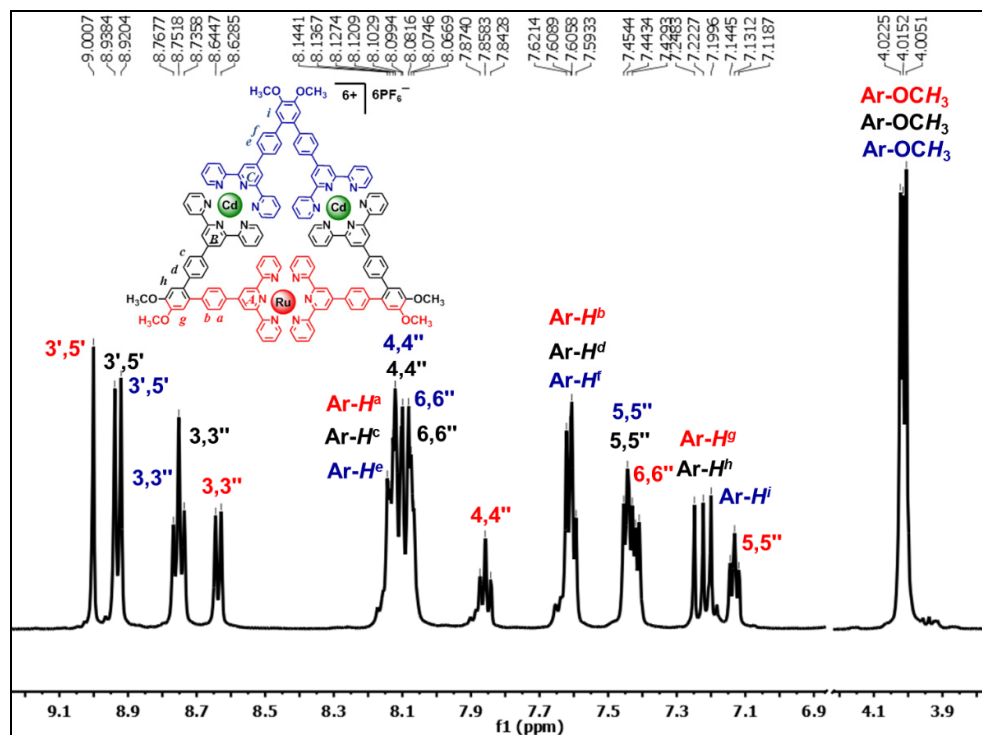


Figure S10: 2D COSY spectrum of isosceles triangle $[(1)(2)(\text{Cd}^{2+})_2](\text{PF}_6^-)_6$ (**8**)

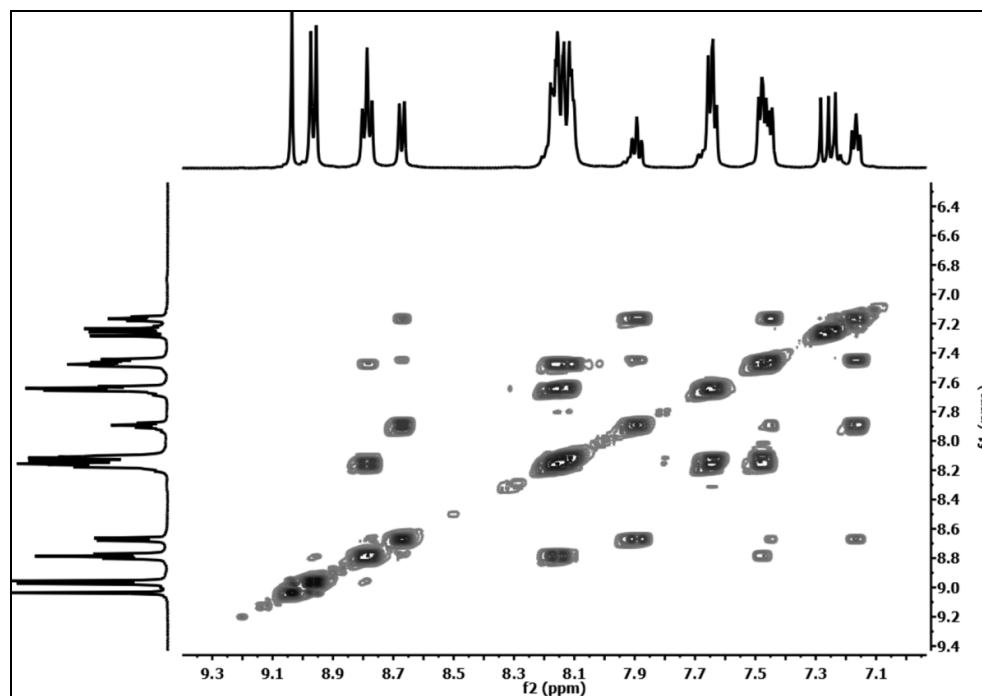


Figure S11: 2D NOESY spectrum of isosceles triangle [(1)(2)(Cd²⁺)₂] (PF₆⁻)₆ (**8**)

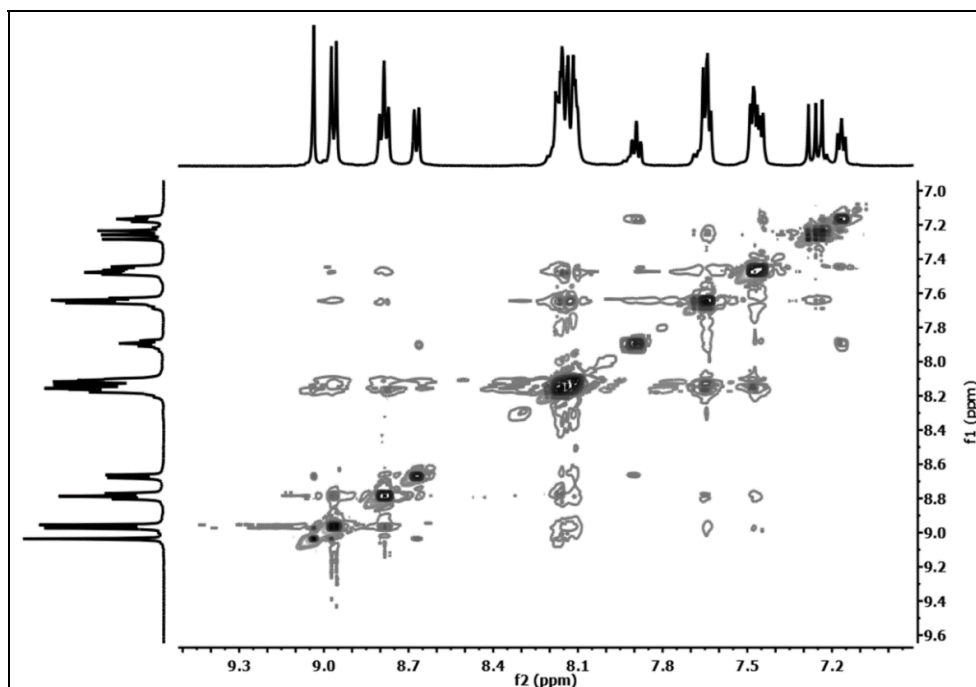


Figure S12: ¹³C NMR spectrum of isosceles triangle [(1)(2)(Cd²⁺)₂] (PF₆⁻)₆ (**8**)

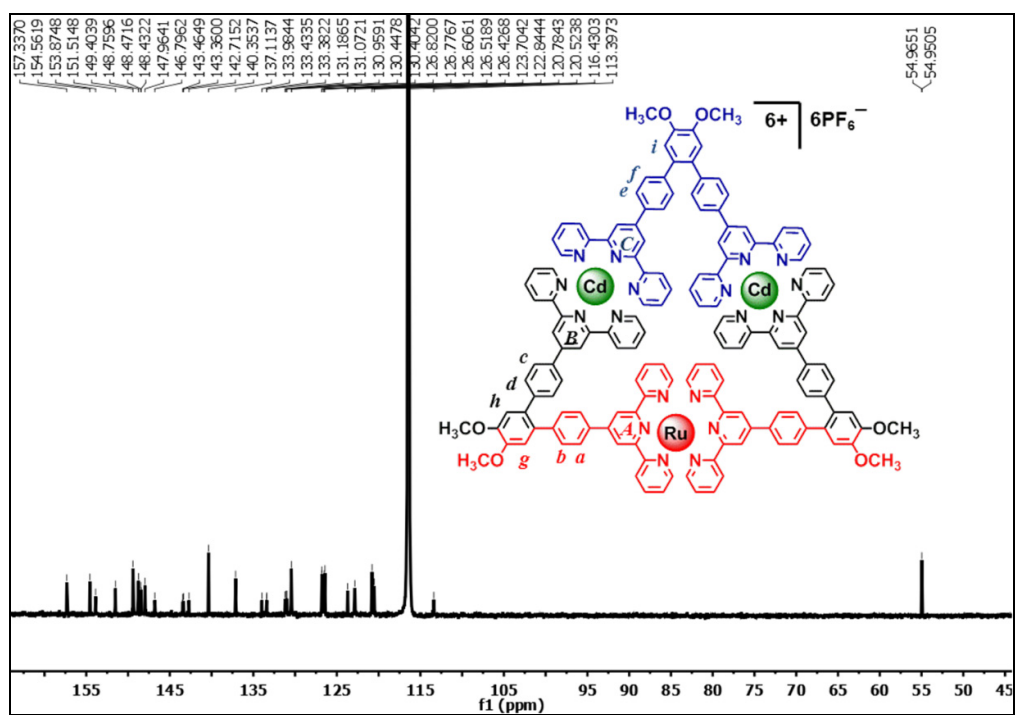


Figure S13: Stacked ^1H NMR spectra (500 MHz) of triangle **3** (top) and tetramer **5** (bottom) and of bimetallic triangle **7** in CD_3CN

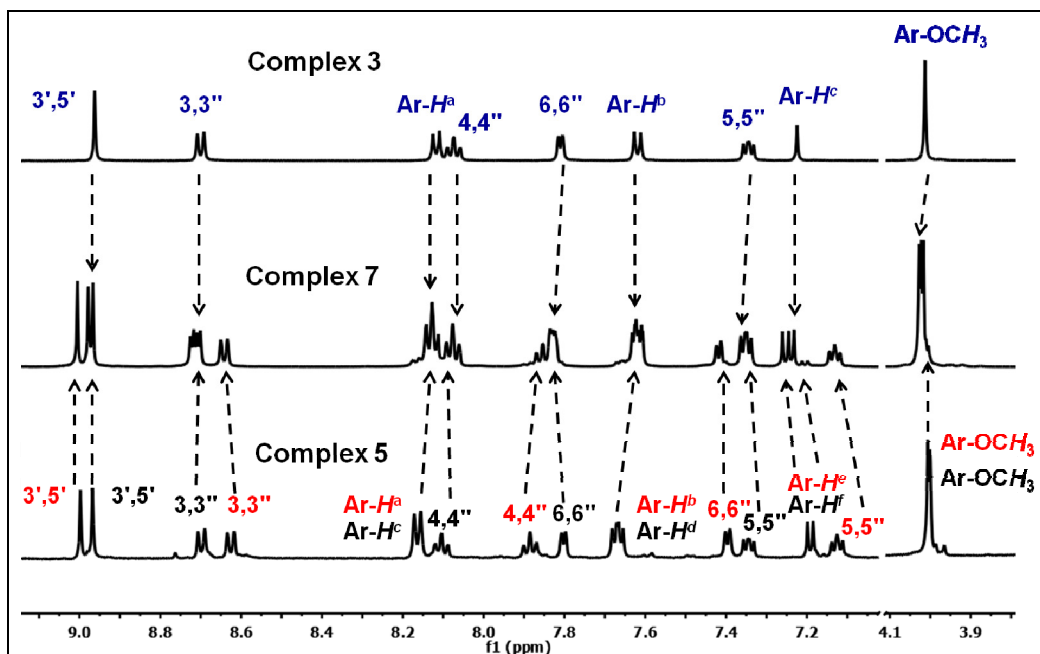


Figure S14: Stacked ^1H NMR spectra (500 MHz) of triangle **4** (top) and tetramer **6** (bottom) and of bimetallic triangle **8** in CD_3CN

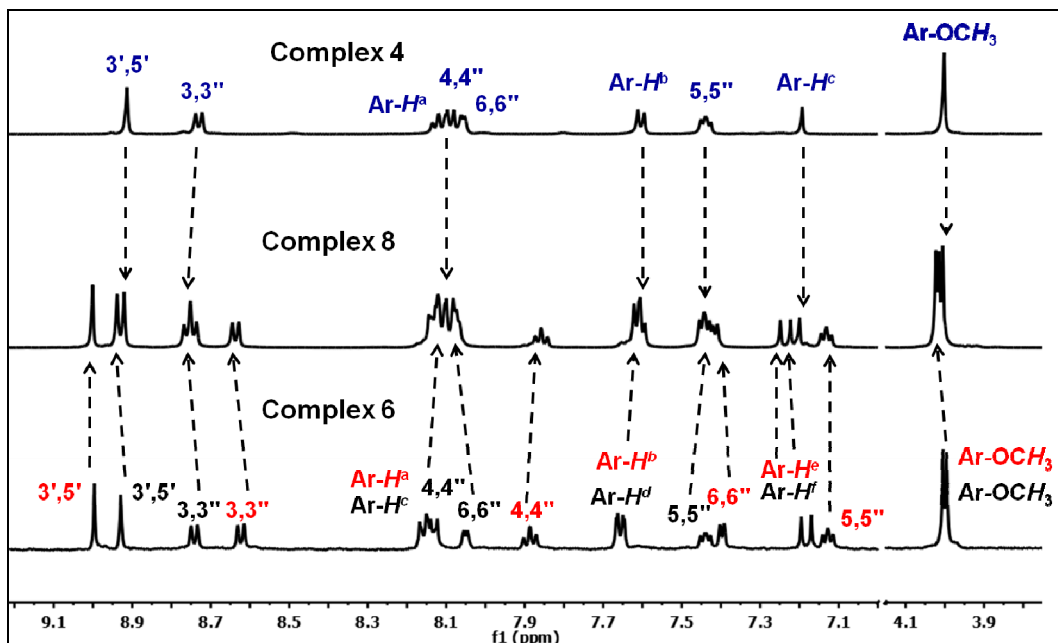


Figure S15: Stacked ^1H NMR spectra (500 MHz) of titration of triangle **3** with tetramer **5** in CD_3CN

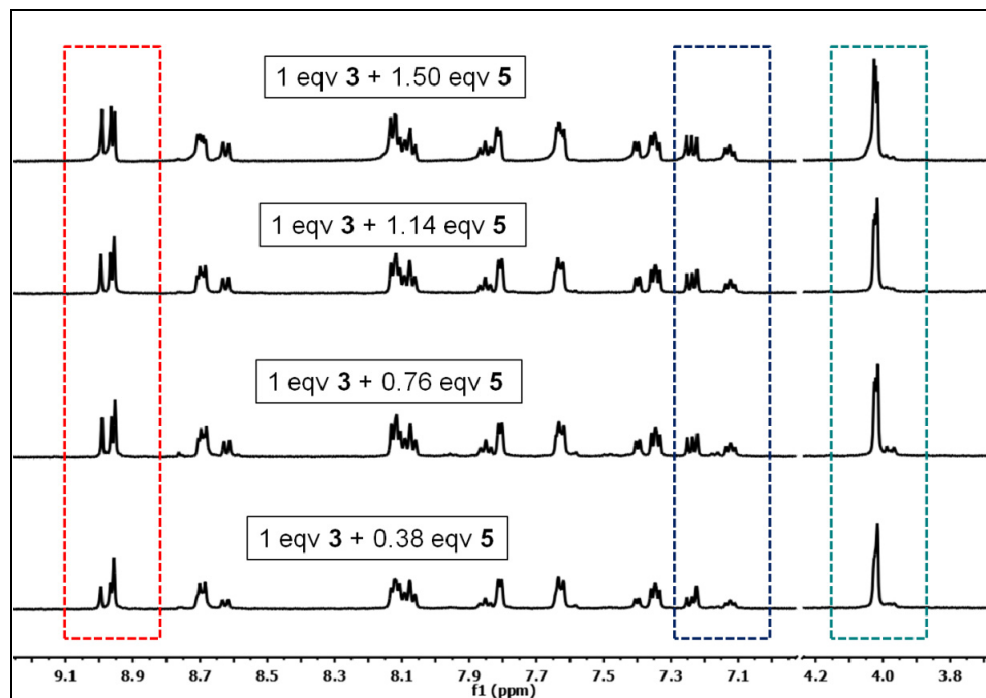


Figure S16: Stacked ^1H NMR spectra (500 MHz) of titration of triangle **4** with tetramer **6** in CD_3CN

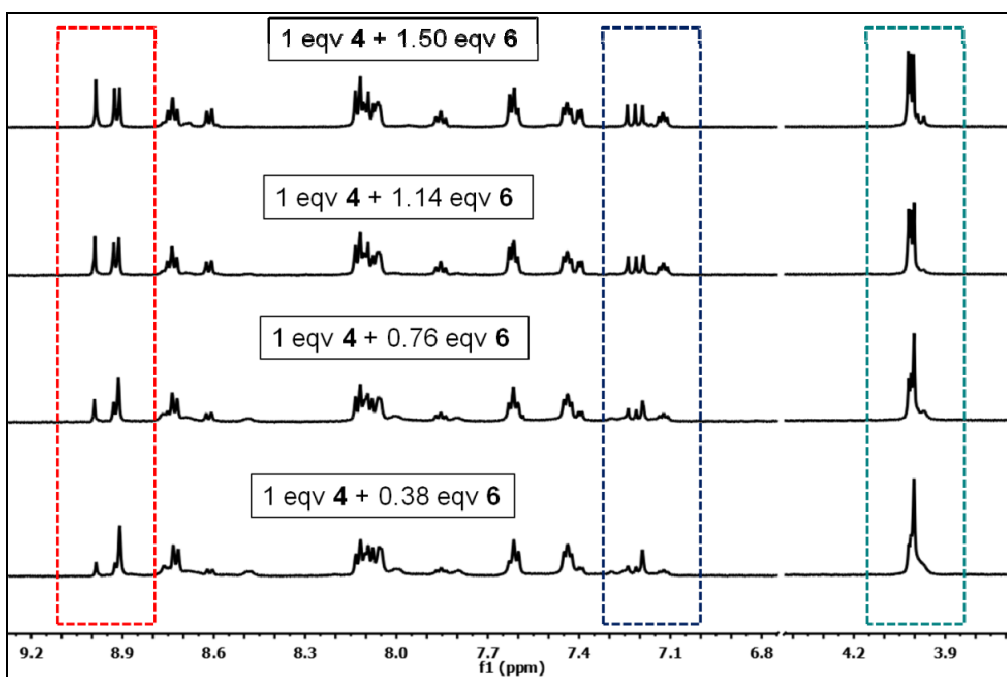


Figure S17: ESI-MS spectrum of bimetallic triangle [(1)(2)(Zn²⁺)₂] (PF₆⁻)₆ (7)

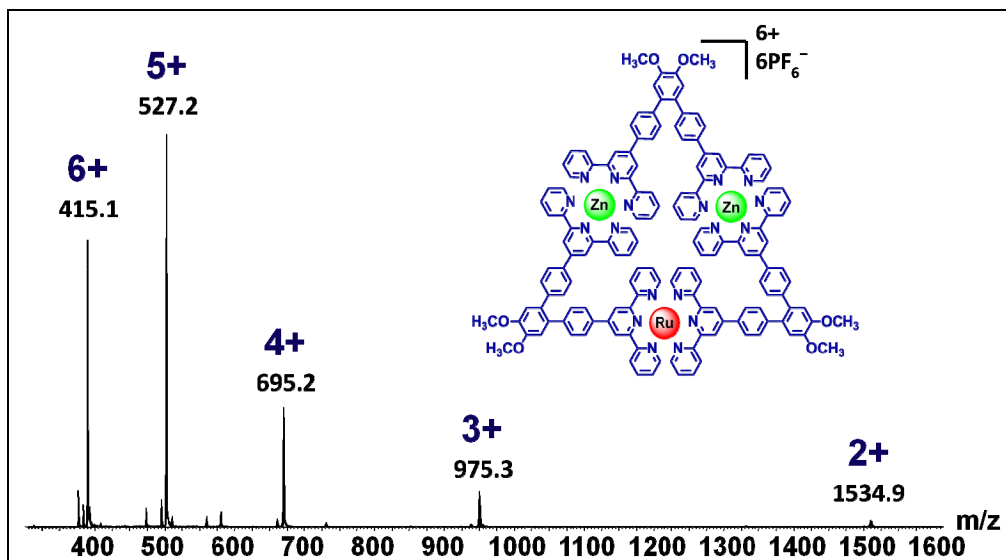


Figure S18: 2D ESI-TWIM-MS spectrum of bimetallic triangle [(1)(2)(Zn²⁺)₂] (PF₆⁻)₆ (7)

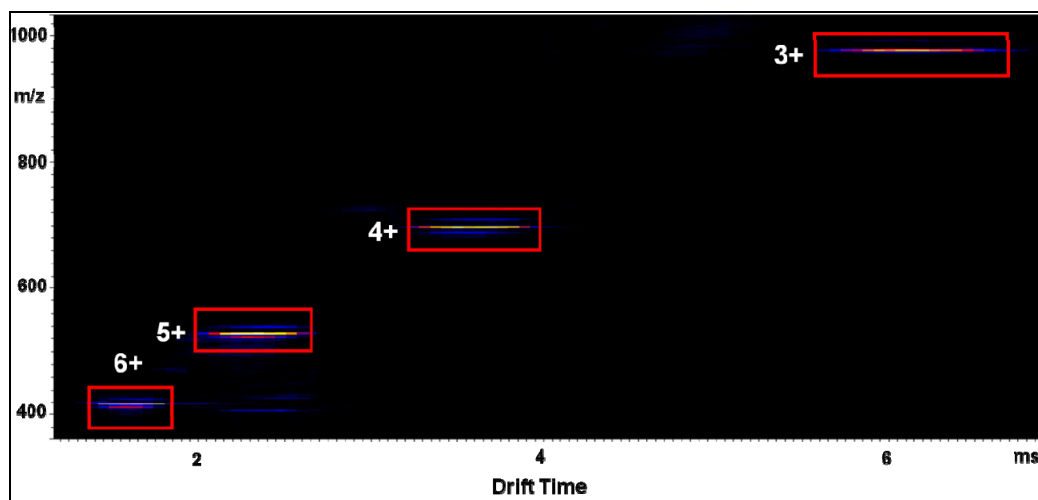


Figure S19: ESI-MS spectrum of bimetallic triangle [(1)(2)(Cd²⁺)₂] (PF₆⁻)₆ (**8**)

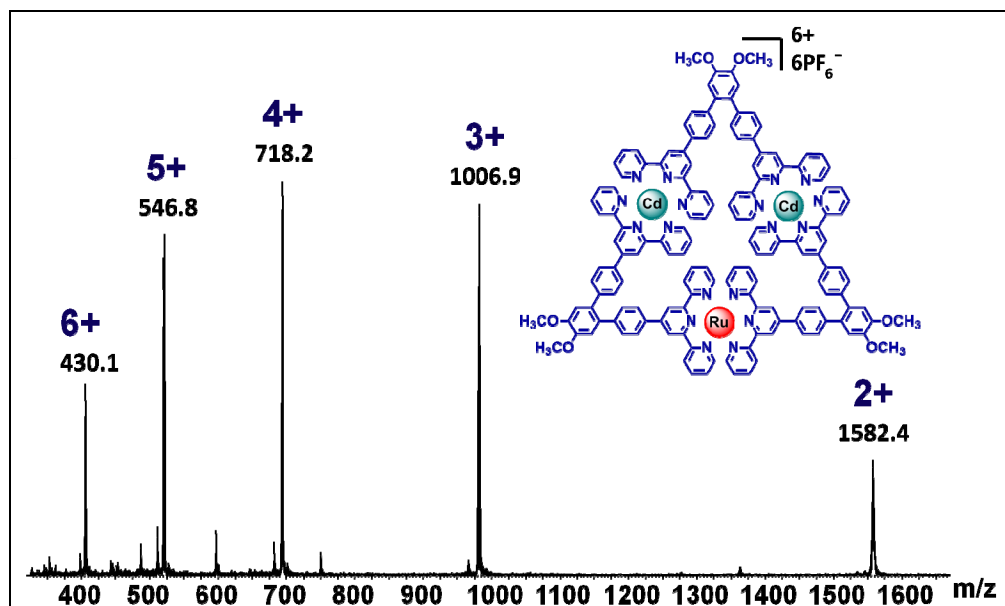


Figure S20: 2D ESI-TWIM-MS spectrum of bimetallic triangle [(1)(2)(Cd²⁺)₂] (PF₆⁻)₆ (**8**)

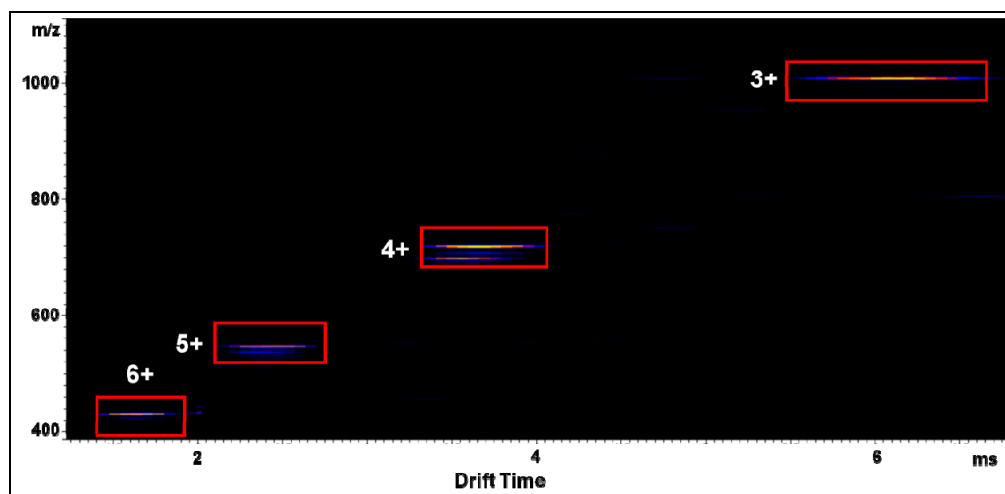


Figure S21: ESI TWIM-gMS² plot of the 5+ charge state of bimetallic triangle [(1)(2)(Zn²⁺)₂](PF₆⁻)₆ (7)

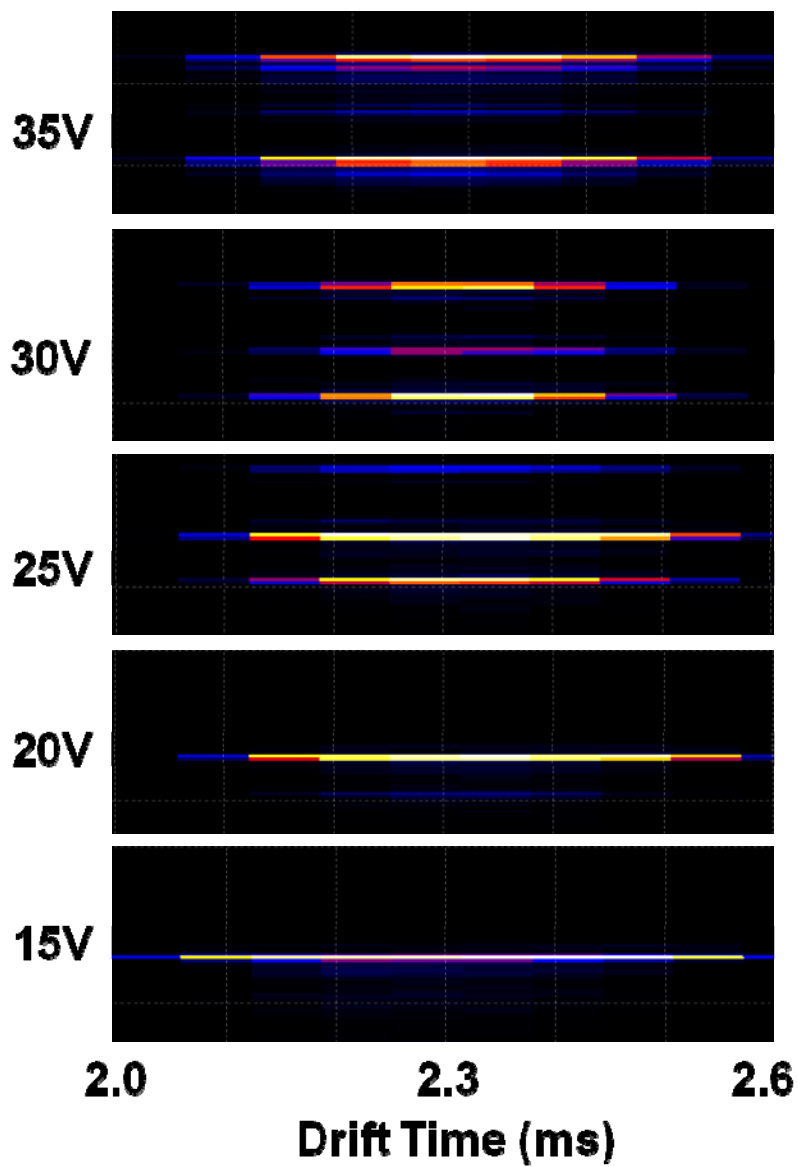
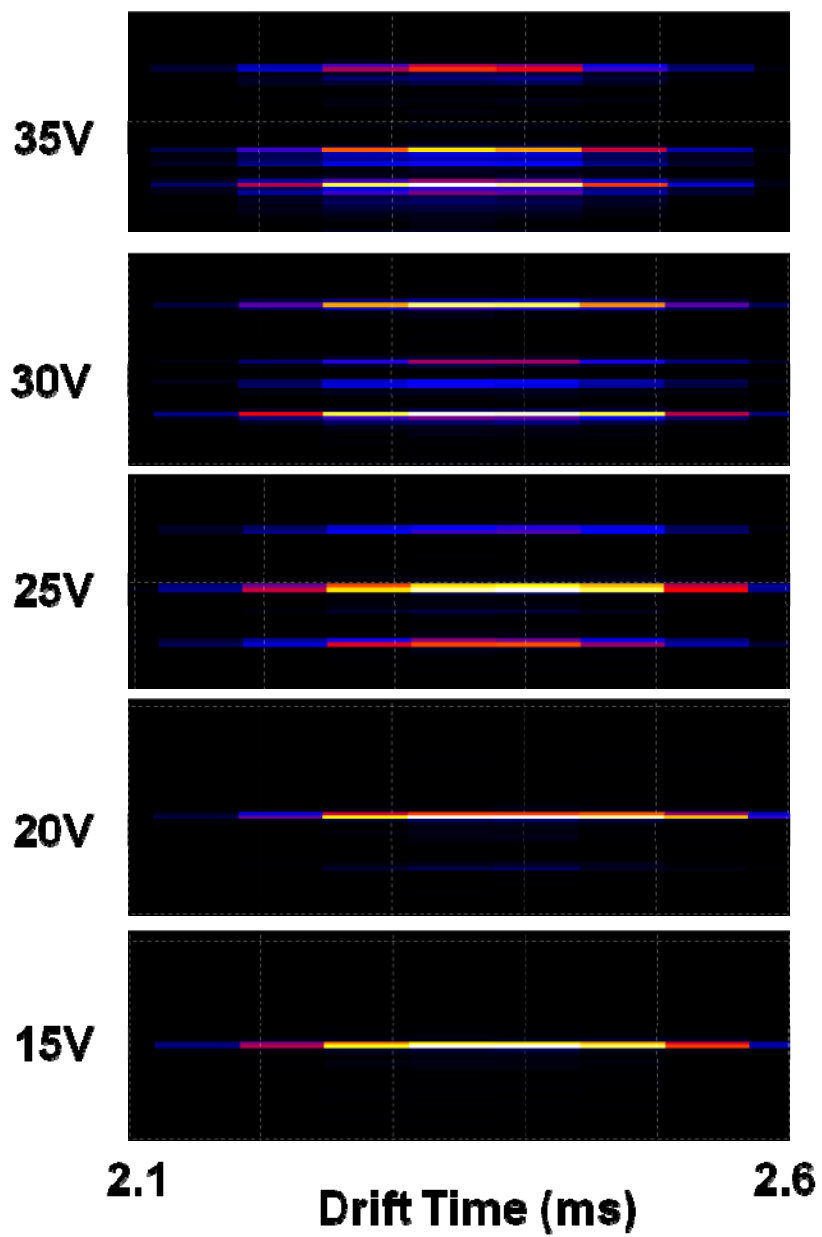


Figure S22: ESI TWIM-gMS² plot of the 5+ charge state of bimetallic triangle [(1)(2)(Cd²⁺)₂] (PF₆⁻)₆ (8)



References:

- [1] A. Schultz, Y. Cao, M. Huang, S. Z. D. Cheng, X. Li, C. N. Moorefield, C. Wesdemiotis, G. R. Newkome, *Dalton Trans.* **2012**, *41*, 11573.
- [2] A. Schultz, X. Li, C. E. McCusker, C. N. Moorefield, F. N. Castellano, C. Wesdemiotis, G. R. Newkome, *Chem. Eur. J.* **2012**, *18*, 11569.
- [3] R. Sarkar, K. Guo, C. N. Moorefield, M. J. Saunders, C. Wesdemiotis, G. R. Newkome, *Angew. Chem. Int. Ed.* **2014**, *53*, 12182.
- [4] A. Schultz, X. Li, C. N. Moorefield, C. Wesdemiotis, G. R. Newkome, *Eur. J. Inorg. Chem.* **2013**, 2492.